DESY-98-069
June 1998

Search for Selectron and Squark Production in e^+p Collisions at HERA

ZEUS Collaboration

Abstract

We have searched for the production of a selectron and a squark in e^+p collisions at a center-of-mass energy of 300 GeV using the ZEUS detector at HERA. The selectron and squark are sought in the direct decay into the lightest neutralino in the framework of supersymmetric extensions to the Standard Model which conserve R-parity. No evidence for the production of supersymmetric particles has been found in a data sample corresponding to 46.6 pb^{-1} of integrated luminosity. We express upper limits on the product of the cross section times the decay branching ratios as excluded regions in the parameter space of the Minimal Supersymmetric Standard Model.

The ZEUS Collaboration

J. Breitweg, M. Derrick, D. Krakauer, S. Magill, D. Mikunas, B. Musgrave, J. Repond, R. Stanek, R.L. Talaga, R. Yoshida, H. Zhang
Argonne National Laboratory, Argonne, IL, USA [p]

M.C.K. Mattingly
Andrews University, Berrien Springs, MI, USA

F. Anselmo, P. Antonioli, G. Bari, M. Basile, L. Bellagamba, D. Boscherini, A. Bruni, G. Bruni, G. Cara Romeo, G. Castellini[1], L. Cifarelli[2], F. Cindolo, A. Contin, N. Coppola, M. Corradi, S. De Pasquale, P. Giusti, G. Iacobucci, G. Laurenti, G. Levi, A. Margotti, T. Massam, R. Nania, F. Palmonari, A. Pesci, A. Polini, G. Sartorelli, Y. Zamora Garcia[3], A. Zichichi
University and INFN Bologna, Bologna, Italy [f]

C. Amelung, A. Bornheim, I. Brock, K. Coböken, J. Crittenden, R. Deffner, M. Eckert, M. Grothe[4], H. Hartmann, K. Heinloth, L. Heinz, E. Hilger, H.-P. Jakob, A. Kappes, U.F. Katz, R. Kerger, E. Paul, M. Pfeiffer, J. Stamm[5], H. Wieber
Physikalisches Institut der Universität Bonn, Bonn, Germany [c]

D.S. Bailey, S. Campbell-Robson, W.N. Cottingham, B. Foster, R. Hall-Wilton, G.P. Heath, H.F. Heath, J.D. McFall, D. Piccioni, D.G. Roff, R.J. Tapper
H.H. Wills Physics Laboratory, University of Bristol, Bristol, U.K. [o]

M. Capua, L. Iannotti, A. Mastroberardino, M. Schioppa, G. Susinno
Calabria University, Physics Dept.and INFN, Cosenza, Italy [f]

J.Y. Kim, J.H. Lee, I.T. Lim, M.Y. Pac[6]
Chonnam National University, Kwangju, Korea [h]

A. Caldwell[7], N. Cartiglia, Z. Jing, W. Liu, B. Mellado, J.A. Parsons, S. Ritz[8], S. Sampson, F. Sciulli, P.B. Straub, Q. Zhu
Columbia University, Nevis Labs., Irvington on Hudson, N.Y., USA [q]

P. Borzemski, J. Chwastowski, A. Eskreys, J. Figiel, K. Klimek, M.B. Przybycień, L. Zawiejski
Inst. of Nuclear Physics, Cracow, Poland [j]

L. Adamczyk[9], B. Bednarek, M. Bukowy, A.M. Czermak, K. Jeleń, D. Kisielewska, T. Kowalski,
M. Przybycień, E. Rulikowska-Zarębska, L. Suszycki, J. Zając
Faculty of Physics and Nuclear Techniques, Academy of Mining and Metallurgy, Cracow, Poland [j]

Z. Duliński, A. Kotański
Jagellonian Univ., Dept. of Physics, Cracow, Poland [k]

G. Abbiendi[10], L.A.T. Bauerdick, U. Behrens, H. Beier[11], J.K. Bienlein, K. Desler, G. Drews, U. Fricke, I. Gialas[12], F. Goebel, P. Göttlicher, R. Graciani, T. Haas, W. Hain, G.F. Hartner, D. Hasell[13], K. Hebbel, K.F. Johnson[14], M. Kasemann, W. Koch, U. Kötz, H. Kowalski, L. Lindemann, B. Löhr, M. Martínez, J. Milewski, M. Milite, T. Monteiro[15], D. Notz, A. Pellegrino, F. Pelucchi, K. Piotrzkowski, M. Rohde, J. Roldán[16], J.J. Ryan[17], P.R.B. Saull, A.A. Savin, U. Schneekloth, O. Schwarzer, F. Selonke, S. Stonjek, B. Surrow[18], E. Tassi, D. Westphal[19], G. Wolf, U. Wollmer, C. Youngman, W. Zeuner
Deutsches Elektronen-Synchrotron DESY, Hamburg, Germany

B.D. Burow, C. Coldewey, H.J. Grabosch, A. Meyer, S. Schlenstedt
DESY-IfH Zeuthen, Zeuthen, Germany

G. Barbagli, E. Gallo, P. Pelfer
University and INFN, Florence, Italy [f]

G. Maccarrone, L. Votano
INFN, Laboratori Nazionali di Frascati, Frascati, Italy [f]

A. Bamberger, S. Eisenhardt, P. Markun, H. Raach, T. Trefzger[20], S. Wölfle
Fakultät für Physik der Universität Freiburg i.Br., Freiburg i.Br., Germany [c]

J.T. Bromley, N.H. Brook, P.J. Bussey, A.T. Doyle[21], S.W. Lee, N. Macdonald, G.J. McCance, D.H. Saxon,
L.E. Sinclair, I.O. Skillicorn, E. Strickland, R. Waugh
Dept. of Physics and Astronomy, University of Glasgow, Glasgow, U.K. [o]

I. Bohnet, N. Gendner, U. Holm, A. Meyer-Larsen, H. Salehi, K. Wick
Hamburg University, I. Institute of Exp. Physics, Hamburg, Germany [c]

A. Garfagnini, L.K. Gladilin[22], D. Kçira[23], R. Klanner, E. Lohrmann, G. Poelz, F. Zetsche
Hamburg University, II. Institute of Exp. Physics, Hamburg, Germany [c]

T.C. Bacon, I. Butterworth, J.E. Cole, G. Howell, L. Lamberti[24], K.R. Long, D.B. Miller, N. Pavel, A. Prinias[25], J.K. Sedgbeer, D. Sideris, R. Walker
Imperial College London, High Energy Nuclear Physics Group, London, U.K. [o]

U. Mallik, S.M. Wang, J.T. Wu[26]
University of Iowa, Physics and Astronomy Dept., Iowa City, USA [p]

P. Cloth, D. Filges
Forschungszentrum Jülich, Institut für Kernphysik, Jülich, Germany

J.I. Fleck[18], T. Ishii, M. Kuze, I. Suzuki[27], K. Tokushuku, S. Yamada, K. Yamauchi, Y. Yamazaki[28]
Institute of Particle and Nuclear Studies, KEK, Tsukuba, Japan [g]

S.J. Hong, S.B. Lee, S.W. Nam[29], S.K. Park
Korea University, Seoul, Korea [h]

H. Lim, I.H. Park, D. Son
Kyungpook National University, Taegu, Korea [h]

F. Barreiro, J.P. Fernández, G. García, C. Glasman[30], J.M. Hernández, L. Hervás[18], L. Labarga, J. del Peso, J. Puga, J. Terrón, J.F. de Trocóniz
Univer. Autónoma Madrid, Depto de Física Teórica, Madrid, Spain [n]

F. Corriveau, D.S. Hanna, J. Hartmann, L.W. Hung, W.N. Murray, A. Ochs, M. Riveline, D.G. Stairs, M. St-Laurent, R. Ullmann
McGill University, Dept. of Physics, Montréal, Québec, Canada [a], [b]

T. Tsurugai
Meiji Gakuin University, Faculty of General Education, Yokohama, Japan

V. Bashkirov, B.A. Dolgoshein, A. Stifutkin
Moscow Engineering Physics Institute, Moscow, Russia [l]

G.L. Bashindzhagyan, P.F. Ermolov, Yu.A. Golubkov, L.A. Khein, N.A. Korotkova, I.A. Korzhavina, V.A. Kuzmin, O.Yu. Lukina, A.S. Proskuryakov, L.M. Shcheglova[31], A.N. Solomin[31], S.A. Zotkin
Moscow State University, Institute of Nuclear Physics, Moscow, Russia [m]

C. Bokel, M. Botje, N. Brümmer, J. Engelen, E. Koffeman, P. Kooijman, A. van Sighem, H. Tiecke, N. Tuning, W. Verkerke, J. Vossebeld, L. Wiggers, E. de Wolf
NIKHEF and University of Amsterdam, Amsterdam, Netherlands [i]

D. Acosta[32], B. Bylsma, L.S. Durkin, J. Gilmore, C.M. Ginsburg, C.L. Kim, T.Y. Ling, P. Nylander, T.A. Romanowski[33]
Ohio State University, Physics Department, Columbus, Ohio, USA [p]

H.E. Blaikley, R.J. Cashmore, A.M. Cooper-Sarkar, R.C.E. Devenish, J.K. Edmonds, J. Große-Knetter[34], N. Harnew, C. Nath, V.A. Noyes[35], A. Quadt, O. Ruske, J.R. Tickner[36], R. Walczak, D.S. Waters
Department of Physics, University of Oxford, Oxford, U.K. [o]

A. Bertolin, R. Brugnera, R. Carlin, F. Dal Corso, U. Dosselli, S. Limentani, M. Morandin, M. Posocco, L. Stanco, R. Stroili, C. Voci
Dipartimento di Fisica dell' Università and INFN, Padova, Italy [f]

J. Bulmahn, B.Y. Oh, J.R. Okrasiński, W.S. Toothacker, J.J. Whitmore
Pennsylvania State University, Dept. of Physics, University Park, PA, USA [q]

Y. Iga
Polytechnic University, Sagamihara, Japan [g]

G. D'Agostini, G. Marini, A. Nigro, M. Raso
Dipartimento di Fisica, Univ. 'La Sapienza' and INFN, Rome, Italy [f]

J.C. Hart, N.A. McCubbin, T.P. Shah
Rutherford Appleton Laboratory, Chilton, Didcot, Oxon, U.K. [o]

D. Epperson, C. Heusch, J.T. Rahn, H.F.-W. Sadrozinski, A. Seiden, R. Wichmann, D.C. Williams
University of California, Santa Cruz, CA, USA [p]

H. Abramowicz[37], G. Briskin[38], S. Dagan[39], S. Kananov[39], A. Levy[39]
Raymond and Beverly Sackler Faculty of Exact Sciences, School of Physics, Tel-Aviv University,
Tel-Aviv, Israel [e]

T. Abe, T. Fusayasu, M. Inuzuka, K. Nagano, K. Umemori, T. Yamashita
Department of Physics, University of Tokyo, Tokyo, Japan [g]

R. Hamatsu, T. Hirose, K. Homma[40], S. Kitamura[41], T. Matsushita
Tokyo Metropolitan University, Dept. of Physics, Tokyo, Japan [g]

M. Arneodo[21], R. Cirio, M. Costa, M.I. Ferrero, S. Maselli, V. Monaco, C. Peroni, M.C. Petrucci, M. Ruspa, R. Sacchi, A. Solano, A. Staiano
Università di Torino, Dipartimento di Fisica Sperimentale and INFN, Torino, Italy [f]

M. Dardo
II Faculty of Sciences, Torino University and INFN - Alessandria, Italy [f]

D.C. Bailey, C.-P. Fagerstroem, R. Galea, K.K. Joo, G.M. Levman, J.F. Martin R.S. Orr, S. Polenz, A. Sabetfakhri, D. Simmons
University of Toronto, Dept. of Physics, Toronto, Ont., Canada [a]

J.M. Butterworth, C.D. Catterall, M.E. Hayes, E.A. Heaphy, T.W. Jones, J.B. Lane, R.L. Saunders, M.R. Sutton, M. Wing
University College London, Physics and Astronomy Dept., London, U.K. [o]

J. Ciborowski, G. Grzelak[42], M. Kasprzak, R.J. Nowak, J.M. Pawlak, R. Pawlak, B. Smalska,
T. Tymieniecka, A.K. Wróblewski, J.A. Zakrzewski, A.F. Żarnecki
Warsaw University, Institute of Experimental Physics, Warsaw, Poland [j]

M. Adamus
Institute for Nuclear Studies, Warsaw, Poland [j]

O. Deppe, Y. Eisenberg[39], D. Hochman, U. Karshon[39]
Weizmann Institute, Department of Particle Physics, Rehovot, Israel [d]

W.F. Badgett, D. Chapin, R. Cross, S. Dasu, C. Foudas, R.J. Loveless, S. Mattingly, D.D. Reeder, W.H. Smith, A. Vaiciulis, M. Wodarczyk
University of Wisconsin, Dept. of Physics, Madison, WI, USA [p]

A. Deshpande, S. Dhawan, V.W. Hughes
Yale University, Department of Physics, New Haven, CT, USA [p]

S. Bhadra, W.R. Frisken, M. Khakzad, W.B. Schmidke
York University, Dept. of Physics, North York, Ont., Canada [a]

[1] also at IROE Florence, Italy
[2] now at Univ. of Salerno and INFN Napoli, Italy
[3] supported by Worldlab, Lausanne, Switzerland
[4] now at University of California, Santa Cruz, USA
[5] now at C. Plath GmbH, Hamburg
[6] now at Dongshin University, Naju, Korea
[7] also at DESY
[8] Alfred P. Sloan Foundation Fellow
[9] supported by the Polish State Committee for Scientific Research, grant No. 2P03B14912
[10] now at INFN Bologna
[11] now at Innosoft, Munich, Germany
[12] now at Univ. of Crete, Greece, partially supported by DAAD, Bonn - Kz. A/98/16764
[13] now at Massachusetts Institute of Technology, Cambridge, MA, USA
[14] visitor from Florida State University
[15] supported by European Community Program PRAXIS XXI
[16] now at IFIC, Valencia, Spain
[17] now a self-employed consultant
[18] now at CERN
[19] now at Bayer A.G., Leverkusen, Germany
[20] now at ATLAS Collaboration, Univ. of Munich
[21] also at DESY and Alexander von Humboldt Fellow at University of Hamburg
[22] on leave from MSU, supported by the GIF, contract I-0444-176.07/95
[23] supported by DAAD, Bonn - Kz. A/98/12712
[24] supported by an EC fellowship
[25] PPARC Post-doctoral fellow
[26] now at Applied Materials Inc., Santa Clara
[27] now at Osaka Univ., Osaka, Japan
[28] supported by JSPS Postdoctoral Fellowships for Research Abroad
[29] now at Wayne State University, Detroit
[30] supported by an EC fellowship number ERBFMBICT 972523
[31] partially supported by the Foundation for German-Russian Collaboration DFG-RFBR (grant no. 436 RUS 113/248/3 and no. 436 RUS 113/248/2)
[32] now at University of Florida, Gainesville, FL, USA
[33] now at Department of Energy, Washington
[34] supported by the Feodor Lynen Program of the Alexander von Humboldt foundation
[35] Glasstone Fellow
[36] now at CSIRO, Lucas Heights, Sydney, Australia
[37] an Alexander von Humboldt Fellow at University of Hamburg
[38] now at Brown University, Providence, RI, USA
[39] supported by a MINERVA Fellowship
[40] now at ICEPP, Univ. of Tokyo, Tokyo, Japan
[41] present address: Tokyo Metropolitan College of Allied Medical Sciences, Tokyo 116, Japan
[42] supported by the Polish State Committee for Scientific Research, grant No. 2P03B09308

[a] supported by the Natural Sciences and Engineering Research Council of Canada (NSERC)
[b] supported by the FCAR of Québec, Canada
[c] supported by the German Federal Ministry for Education and Science, Research and Technology (BMBF), under contract numbers 057BN19P, 057FR19P, 057HH19P, 057HH29P
[d] supported by the MINERVA Gesellschaft für Forschung GmbH, the German Israeli Foundation, the U.S.-Israel Binational Science Foundation, and by the Israel Ministry of Science
[e] supported by the German-Israeli Foundation, the Israel Science Foundation, the U.S.-Israel Binational Science Foundation, and by the Israel Ministry of Science
[f] supported by the Italian National Institute for Nuclear Physics (INFN)
[g] supported by the Japanese Ministry of Education, Science and Culture (the Monbusho) and its grants for Scientific Research
[h] supported by the Korean Ministry of Education and Korea Science and Engineering Foundation
[i] supported by the Netherlands Foundation for Research on Matter (FOM)
[j] supported by the Polish State Committee for Scientific Research, grant No. 115/E-343/SPUB/P03/002/97, 2P03B10512, 2P03B10612, 2P03B14212, 2P03B10412
[k] supported by the Polish State Committee for Scientific Research (grant No. 2P03B08614) and Foundation for Polish-German Collaboration
[l] partially supported by the German Federal Ministry for Education and Science, Research and Technology (BMBF)
[m] supported by the Fund for Fundamental Research of Russian Ministry for Science and Education and by the German Federal Ministry for Education and Science, Research and Technology (BMBF)
[n] supported by the Spanish Ministry of Education and Science through funds provided by CICYT
[o] supported by the Particle Physics and Astronomy Research Council
[p] supported by the US Department of Energy
[q] supported by the US National Science Foundation

1 Introduction

Supersymmetry (SUSY) theories relate bosons and fermions by associating to each fermion a bosonic partner and vice-versa. Among the appealing consequences of this symmetry is the cancellation of quadratic divergences occurring in the scalar Higgs sector of the Standard Model (SM) and models beyond the SM [1]. There is, on the other hand, no experimental evidence for SUSY. Since supersymmetric particles are not observed at the masses of their standard partners, SUSY would need to be broken.

In the supersymmetric extension of the SM known as the Minimal Supersymmetric Standard Model (MSSM), the supersymmetry-breaking terms are added by hand, generating a model with many free parameters (for a review and the original references see [2]). In this model the breaking of $\mathrm{SU}(2) \times \mathrm{U}(1)_{\mathrm{Y}}$ is generated through the vacuum expectation values v_1 and v_2 of two Higgs doublets, which give masses to the down-type quarks and charged leptons (v_1) and to the up-type quarks (v_2). Selectrons ($\tilde{e}_{\mathrm{L}}$, $\tilde{e}_{\mathrm{R}}$) and squarks ($\tilde{q}^{\mathrm{f}}_{\mathrm{L}}$, $\tilde{q}^{\mathrm{f}}_{\mathrm{R}}$) are the scalar partners of the left- and right-handed electrons and the quarks of flavor f. The supersymmetric partners of the gauge bosons and the Higgs particles, known as gauginos and higgsinos, mix together giving rise to four neutral mass eigenstates χ^0_i (neutralinos) and two charged mass eigenstates $\chi^{\pm}_j$ (charginos). The masses of the neutralinos depend on the supersymmetry-breaking parameters M_1 and M_2 (for the U(1) and SU(2) gauginos), on the higgsino mass parameter μ and on the ratio of the two Higgs vacuum expectation values $\tan\beta \equiv v_2/v_1$. There is a new multiplicative quantum number, R-parity (R_P), which takes the values +1 for the ordinary particles and -1 for the supersymmetric particles. In models where R_P is conserved, the supersymmetric particles are produced only in pairs and the lightest supersymmetric particle (LSP) is stable. In these models, the production of a slepton and a squark is the lowest order process in which supersymmetric particles could be produced at HERA [3, 4, 5]. Other processes, such as the production of a slepton and a gaugino [6] have a smaller cross section.

We report here on the search for the R_P-conserving production and decay of a selectron [1] and a squark, $e^+p \to \tilde{e}^+_{\mathrm{a}}\tilde{q}^{\mathrm{f}}_{\mathrm{b}}X$ ($\mathrm{a} = \mathrm{L}, \mathrm{R}$, $\mathrm{b} = \mathrm{L}, \mathrm{R}$). This process is mediated by the t-channel exchange of a neutralino, as shown in figure 1. As the production of high-mass particles in the final state involves high Bjorken-x valence quarks from the proton, the process is mostly sensitive to the up quark. This measurement was performed with the ZEUS detector using an integrated luminosity $\mathcal{L} = 46.6\,\mathrm{pb}^{-1}$. The H1 collaboration has published results of a search similar to the one presented in this paper, using an integrated luminosity $\mathcal{L} \simeq 6.4\,\mathrm{pb}^{-1}$ [7].

The selectron (squark) can decay directly to the lightest neutralino, χ^0_1, and a positron (quark): $\tilde{e} \to e\chi^0_1$ ($\tilde{q} \to q\chi^0_1$). Under the assumption that the lightest neutralino is the LSP and that R_P is conserved, one can conclude that the neutralino will escape detection. In this case, the signature for the production of a selectron and a squark is one positron from $\tilde{e}$ decay, a high P_{t} hadronic system from $\tilde{q}$ decay and missing momentum from the two neutralinos [8]. The search for this process is used to set limits on the masses of

[1] Throughout this paper we will call "selectron" the scalar partner of the positron.

the selectron and of the squark for a wide range of values of the MSSM parameters. Limits are derived for all squarks assuming that they are degenerate in mass. We also set limits separately for the $\tilde{u}$ squark. These limits can be considered complementary to the strong limits on the squark mass from $p\bar{p}$ collider experiments [9] that are valid within models with additional constraints compared to the MSSM. The present search leads to limits comparable to those so far obtained from e^+e^- experiments [10, 11] for particular combinations of the $\tilde{e}$ and $\tilde{q}$ masses.

2 Experimental Setup

The $46.6\,\mathrm{pb}^{-1}$ of data used for this analysis were collected with the ZEUS detector at the HERA collider during the years 1994 to 1997. The collider operated at a center-of-mass energy of 300 GeV with positrons of energy $E_e = 27.5\,\mathrm{GeV}$ and protons of energy $E_p = 820\,\mathrm{GeV}$.

The ZEUS detector is described in detail elsewhere [12]. The main subdetectors used in the present analysis are the central tracking detector (CTD) [13] positioned in a 1.43 T solenoidal magnetic field and the compensating uranium-scintillator sampling calorimeter (CAL) [14], subdivided in forward (FCAL), barrel (BCAL) and rear (RCAL) sections. Under test beam conditions the CAL energy resolution is $18\%/\sqrt{E(\mathrm{GeV})}$ for electrons and $35\%/\sqrt{E(\mathrm{GeV})}$ for hadrons. A three-level trigger was used to select events online. The trigger criteria applied relied primarily on the energies deposited in the calorimeter. The trigger decision was based on electromagnetic energy, total transverse energy and missing transverse momentum. Timing cuts were used to reject beam-gas interactions and cosmic rays.

The luminosity was measured to a precision of 1.5% from the rate of energetic bremsstrahlung photons produced in the process $e^+\,p \to e\,p\,\gamma$ [15].

3 Production Model

The amplitude of the process depicted in figure 1 is given by the sum of four exchange graphs, one for each MSSM neutralino. The cross section depends on the MSSM parameters M_1, M_2, μ, $\tan\beta$, and on the masses of the produced particles, $\sigma_{ep\to\tilde{e}_\mathrm{a}\tilde{q}^\mathrm{f}_\mathrm{b}X} = \sigma^\mathrm{f}_\mathrm{ab}(M_1, M_2, \mu, \tan\beta, m_{\tilde{e}_\mathrm{a}}, m_{\tilde{q}^\mathrm{f}_\mathrm{b}})$. The cross section depends to a very good approximation on the sum $m_{\tilde{e}} + m_{\tilde{q}}$ of the scalar particle masses. The branching ratios, B, for the decays $\tilde{e} \to e\chi^0_1$ and $\tilde{q} \to q\chi^0_1$ depend on the same MSSM parameters. Squarks are not allowed to decay to gluinos ($\tilde{g}$) as we assume $m_{\tilde{g}} > m_{\tilde{q}}$.

For $|\mu| < M_1$ and M_2, the χ^0_1 is higgsino-like and the cross sections are small, due to the small coupling constants. In the region $|\mu| > M_1$ and M_2, the χ^0_1 is gaugino-like and good limits on the sparticle masses are possible with the exception of particular combinations

of M_1 and M_2 (for $\mu > 0$) when the LSP becomes a chargino. In the asymptotic region $|\mu| \gg M_2 > M_1$, the mass of the lightest neutralino is $m_{\chi_1^0} \sim M_1$ and the masses of the next-to-lightest neutralino and of the charginos are $m_{\chi_2^0} \sim m_{\chi_1^+} \sim M_2$; therefore for $M_2 > m_{\tilde{e}}$ and $m_{\tilde{q}}$, the scalar particles can only decay to the LSP and $B = 1$, while $B \approx 30\%$ when $M_2 < m_{\tilde{e}}$ and $m_{\tilde{q}}$. In this region the cross section depends weakly on $\tan\beta$. We take $|\mu| = 500\,\mathrm{GeV}$ as an example of large μ values.

To reduce the number of free parameters, the $\tilde{e}_\mathrm{L}$ and $\tilde{e}_\mathrm{R}$ are assumed to have the same mass $m_{\tilde{e}}$, and all the squarks (except $\tilde{t}$ whose contribution can be neglected) to have the same mass $m_{\tilde{q}}$. Alternatively we consider the case that $\tilde{u}$ is the only squark contributing to the process. We assume no mixing between $\tilde{e}_\mathrm{L}$ ($\tilde{q}^\mathrm{f}_\mathrm{L}$) and $\tilde{e}_\mathrm{R}$ ($\tilde{q}^\mathrm{f}_\mathrm{R}$). In Grand Unified Theories (GUT) the gaugino masses unify at the GUT scale which leads, at the electroweak scale, to the relation $M_1 = \frac{5}{3}\tan^2\theta_W\, M_2 \simeq \frac{1}{2}M_2$, which is adopted here to fix the branching ratios and compare with other experiments.

4 Monte Carlo Simulation

Monte Carlo simulations are used to determine the efficiency for selecting the signal, and also to estimate the rate of the SM background. All the signal and background events were passed through the simulation of the detector response based on GEANT [16], incorporating the effects of the trigger. They were subsequently processed with the same reconstruction and analysis programs used for the data.

4.1 Signal

The calculation of the leading-order cross sections and the simulation of the signal have been performed with a Monte Carlo (MC) generator (MSSM, see [17]) based on the calculations of [5]. In the calculation of the total cross section, the proton parton density is modeled using the GRV-LO [18] set. The change of the structure functions to CTEQ-LO [19] and GRV-HO produced variations always less than 4%. The effect of the initial state QED radiation from the incoming lepton was included using the Weizsäcker-Williams approximation. To generate the signal MC samples the MSSM MC is interfaced to ARIADNE [20], which implements the Color Dipole Model (CDM) to simulate the QCD radiation, and JETSET [21], for the fragmentation of the final state partons. The signal samples were generated for 118 different combinations of the values for the masses $m_{\tilde{e}}$, $m_{\tilde{q}}$ and $m_{\chi_1^0}$, by assuming the exchanged neutralino to be a pure photino ($\tilde{\gamma}$), since the event kinematics and the distributions of the decay products are insensitive to the neutralino mixing parameters. The $\tilde{e}$ and $\tilde{q}$ were then forced to decay directly into χ_1^0.

4.2 Background

To evaluate the SM background we considered the following reactions which can mimic the signature for a selectron-squark event:

- neutral current (NC) deep inelastic scattering (DIS) events with missing momentum due to the presence of neutrinos, muons or not-completely-contained hadronic energy;
- charged current (CC) DIS events with a true or fake positron in the final state;
- W production processes which can mimic the signal via the leptonic decays;
- lepton pair production from Bethe-Heitler interactions ($\gamma\gamma \to e^+e^-, \mu^+\mu^-, \tau^+\tau^-$);
- photoproduction with high transverse energy and heavy flavor production, with true or fake positrons in the final state.

Backgrounds from NC and CC DIS events were simulated using HERACLES [22], which includes first order electroweak radiative corrections. The hadronic final states were simulated using LEPTO [23] and JETSET interfaced with HERACLES using DJANGO [24]. QCD radiation was simulated using the CDM as implemented in ARIADNE and, as a cross check, with the exact first order matrix elements followed by parton showering (MEPS option). The production of $W^{\pm}$ was simulated using EPVEC [25]. The production of lepton pairs in both elastic and inelastic Bethe-Heitler interactions is simulated using LPAIR [26]. All these samples correspond to luminosities at least five times larger than that of the data. The photoproduction background was simulated using events with high transverse energy produced in direct- and resolved-photon interactions, which were generated using HERWIG [27]. Samples of heavy flavors ($\bar{c}c$, $\bar{b}b$) were also produced via the boson gluon fusion mechanism, as implemented in AROMA [28]. These last two samples, which represent a small background, correspond to a luminosity comparable to that of the data.

5 Event Selection

The event selection for the SUSY particles search requires the following global event quantities calculated from the reconstructed vertex and the calorimeter measurements:

$$\begin{aligned} E - P_{\mathrm{Z}} &= \sum_{\mathrm{i}} \left(E_{\mathrm{i}} - P_{\mathrm{Z,i}}\right) \\ \not{P}_{\mathrm{t}} &= \sqrt{\left(\textstyle\sum_{\mathrm{i}} P_{\mathrm{X,i}}\right)^2 + \left(\textstyle\sum_{\mathrm{i}} P_{\mathrm{Y,i}}\right)^2} \end{aligned}$$

where $E_{\rm i}$ is the energy measured in the i^{th} calorimeter cell and $\vec{P}_{\rm i} \equiv E_{\rm i}\,\vec{n}_{\rm i}$, with $\vec{n}_{\rm i}$ the unit vector from the reconstructed vertex to the cell center[2]. The sums run over all calorimeter cells. The missing transverse momentum $\not\!\!P_{\rm t}$ and the longitudinal momentum variable $E - P_{\rm Z}$ equal, respectively, zero and twice the incident positron beam energy ($2E_e = 55$ GeV) for fully contained events. The signal events are expected to have large $\not\!\!P_{\rm t}$ and low $E - P_{\rm Z}$ due to the momentum carried away by the escaping neutralinos. The calculation of the hadronic transverse momentum ($P_{\rm t}^{\rm h}$) excludes cells in the calorimeter sum which belong to a cluster which is identified as the candidate positron from $\tilde{e}$ decay.

Events are selected by requiring an identified positron with transverse momentum $P_{\rm t}^{\rm e} > 4$ GeV and a hadronic system with $P_{\rm t}^{\rm h} > 4$ GeV.

Positron candidates were identified using the pattern of energy deposits in CAL [29], which provided the measurement of its energy E_e and angles θ_e, ϕ_e. Additional requirements were applied:

- *isolation*: the total transverse energy not associated with the positron candidate within a cone of radius R=0.8 units in the (η, ϕ) plane around its direction must be less than 3 GeV and the sum of the momenta of the tracks pointing in a cone of radius R=0.8 units in η,ϕ around the positron, excluding the highest momentum track, must be less than 2 GeV. These cuts remove fake positrons from CC and photoproduction that are close to the hadronic jet;
- *track matching*: if the candidate positron is within a region where the tracking efficiency is high, namely $\theta_e > 0.35$ radians, a match with a track is required such that
  - the distance of closest approach between the electromagnetic (EM) cluster and the track extrapolated from the CTD be less than 6 cm,
  - the ratio of the track to CAL transverse momentum, $P_{\rm t}^{\rm track}/P_{\rm t}^{\rm e} > 0.2$,
  - the track has a positive charge or $P_{\rm t}^{\rm track} > 45$ GeV;

  if $\theta_e < 0.35$, the requirement on the candidate positron transverse momentum is raised to $P_{\rm t}^{\rm e} > 10$ GeV;
- *fiducial cut*: polar angle $\theta_e < 2$; this cut eliminates most of the low Q^2 NC DIS background.

To ensure that the selected events come from e^+p interactions we apply standard cosmic ray and beam gas rejection cuts and require a reconstructed vertex within 50 cm of the nominal interaction point along the Z axis.

[2]The ZEUS coordinate system is a right handed system with the Z axis pointing in the proton direction. The pseudorapidity is defined as $\eta = -\ln(\tan\frac{\theta}{2})$, and the polar angle θ is measured with respect to the Z direction.

In figures 2 a) and b) the $\not\!\!P_{\rm t}$ and $E-P_{\rm Z}$ distributions of the data, after a cut $\not\!\!P_{\rm t} > 10\,\mathrm{GeV}$, (full points) are compared with the total background expectation (full line) and with a Monte Carlo signal sample corresponding to the masses $m_{\tilde{e}} = 80\,\mathrm{GeV}$, $m_{\tilde{q}} = 80\,\mathrm{GeV}$ and $m_{\chi_1^0} = 50\,\mathrm{GeV}$ (dotted line). Good agreement is observed between the distributions of the data and the background Monte Carlo.

To determine the values of the final cuts, an optimization procedure was applied, which maximized the ratio ϵ/U for simulated events, where ϵ is the efficiency and U is the 95% confidence level (CL) upper limit on the signal when the number of events found equals the expected background. Events were accepted if they satisfied the following requirements:

- $E - P_{\rm Z} < 50\,\mathrm{GeV}$;
- $\not\!\!P_{\rm t} > 14\,\mathrm{GeV}$;
- $(E - P_{\rm Z})/\not\!\!P_{\rm t} < 1$.

The acceptance for the $e^+\,q\,\chi_1^0\,\chi_1^0$ final state is close to zero for small mass differences $\Delta m = \min(m_{\tilde{e}} - m_{\chi_1^0}, m_{\tilde{q}} - m_{\chi_1^0})$ and reaches a plateau for $\Delta m > 10\,\mathrm{GeV}$. The level of the plateau increases from 25% at $m_{\tilde{e}} = m_{\tilde{q}} = 40\,\mathrm{GeV}$ to about 50% at $m_{\tilde{e}}$ or $m_{\tilde{q}} = 120\,\mathrm{GeV}$. The acceptance was modeled with a two parameter fit as a function of $m_{\chi_1^0}$ for fixed $m_{\tilde{e}}$ and $m_{\tilde{q}}$. Subsequently a bilinear interpolation was used to obtain the parameters at any $m_{\tilde{e}}$ and $m_{\tilde{q}}$.

In figures 2 c), d) and e), the data, the signal sample and the SM background are shown in the $\not\!\!P_{\rm t}$, $E - P_{\rm Z}$ plane, where the final cuts are also drawn. The expected SM background is $1.99^{+0.57}_{-0.84}$ events, as shown in table 1. The systematic uncertainties quoted for the background are evaluated as described in section 6. No photoproduction or heavy flavor event survived the selection. An alternative method was used to confirm that the photoproduction background was not underestimated due to the limited MC statistics. It was found that the rate of photoproduction events passing all of the kinematic cuts (except positron identification) was only a small fraction of the CC background rate. Assuming that the fake positron fraction was the same for CC and photoproduction events, the resulting photoproduction rate was negligible.

One event survived the selection criteria and was identified as containing a high-Q^2 positron with associated $\not\!\!P_{\rm t}$ in the calorimeter due to two muons in the final state.

6 Systematic Uncertainties

The main source of systematic uncertainty on the efficiency ϵ comes from the interpolation between the generated Monte Carlo mass points ($\Delta\epsilon/\epsilon = 6\%$). Other contributions from detector effects that affect both the acceptance and the background are the uncertainties on the positron identification efficiency ($\Delta\epsilon/\epsilon = 1\%$), on the calorimeter energy scales

($\Delta\epsilon/\epsilon = 2\%$), on the efficiency of the matching between a track and an EM cluster ($\Delta\epsilon/\epsilon = 3.5\%$), on the isolation requirements ($\Delta\epsilon/\epsilon = 3\%$) and on the vertex distribution ($\Delta\epsilon/\epsilon = 1\%$). Another common source is the 1.5% uncertainty in the total integrated luminosity of the 1994-1997 e^+p data sample. We quote an overall systematic uncertainty $\Delta\epsilon/\epsilon = 8.5\%$.

In addition to the experimental sources, effects due to the different treatment of the QCD radiation in the final state for the CC and NC background were evaluated using Monte Carlo samples generated with the MEPS option. The variation of the CC background was found to be below the statistical uncertainty. No NC MEPS event survived the final selection. This difference with respect to the ARIADNE NC background is included as a systematic uncertainty. The theoretical uncertainties on the cross sections of the background processes are also included in table 1. The quoted errors are due to uncertainties on: the proton parton distribution functions (pdf) for the NC and CC backgrounds ($5-6\%$), the missing higher orders and proton and photon pdf for W production (35%) and the uncertainties mainly due to inelastic contributions on the lepton pair production (10%). The total error on the background ($\sim \pm 35\%$) is taken to be the sum in quadrature of the statistical and systematic errors. For the estimated background and one observed event this $\sim 35\%$ variation of the background normalization results in a 4% variation of the 95% CL upper limit on the number of signal events.

7 Results

The event found in the data sample is compatible with the expected SM background. Therefore we derive upper limits on the $\tilde{e}$,$\tilde{q}$ production cross section times the branching ratios ($\sigma \times B$) for the decay to the lightest neutralino χ_1^0. The 95% CL upper limit on the signal, including the systematic uncertainty on the acceptance and the uncertainty in the background as described in [30], is $N_{\rm UL} = 3.9$ events. The 95% CL upper limit on $\sigma \times B$ is obtained as a function of the selectron, squark and neutralino masses through $\sigma \times B < N_{\rm UL}/\epsilon\mathcal{L}$, where $\epsilon = \epsilon(m_{\tilde{e}}, m_{\tilde{q}}, m_{\chi_1^0})$ is the parametrized efficiency and $\mathcal{L}$ is the integrated luminosity. Figures 3 a) and b) show the upper limit on $\sigma \times B$ in the plane defined by $m_{\tilde{e}}$ and $m_{\tilde{q}}$ for two values of $m_{\chi_1^0}$ (35 and 50 GeV). At high $m_{\tilde{e}}$ and $m_{\tilde{q}}$ and large Δm we exclude $\sigma \times B > 0.21\,$pb. For $m_{\chi_1^0} \leq 50$ GeV, $\Delta m > 10\,$GeV and $(m_{\tilde{e}} + m_{\tilde{q}})/2 > 70$ GeV we exclude $\sigma \times B > 0.25\,$pb. For any mass combination with $\Delta m > 10\,$GeV we exclude $\sigma \times B > 0.5\,$pb.

From the comparison of the upper limit on $\sigma \times B$ with the theoretical value from the model calculations we derive exclusion areas in the parameter space of the MSSM. The theoretical cross sections were evaluated by taking into account the complete neutralino mixing and the branching ratios for the decays of $\tilde{e}$ and $\tilde{q}$ to χ_1^0, computed at the tree level. The cross section times branching ratios is computed from:

$$(\sigma \times B)_{\rm th} = \sum_{\rm a,b=L,R} \sum_{\rm f=1}^{5} \{\ \sigma_{e^+p \to \tilde{e}_{\rm a}\tilde{q}^{\rm f}_{\rm b}}\, B(\tilde{e}^+_{\rm a} \to e^+\chi_1^0)\, B(\tilde{q}^{\rm f}_{\rm b} \to q^{\rm f}\chi_1^0) +$$

$$\sigma_{e^+p\to\tilde{e}_a\bar{\tilde{q}}^f_b}\, B(\tilde{e}^+_a \to e^+\chi^0_1)\, B(\bar{\tilde{q}}^f_b \to \bar{q}^f\chi^0_1)\,\}.$$

In figures 3 c) and d) we show the excluded regions in the plane defined by the lightest neutralino and by $(m_{\tilde{e}} + m_{\tilde{q}})/2$. The cross section for the $\tilde{e}$ and $\tilde{q}$ production depends mainly on the sum of the two masses; we give the excluded region for $m_{\tilde{e}} = m_{\tilde{q}}$ since the efficiency and the branching ratios depend separately on the two masses. The limits are shown for $\mu = \pm 500$ GeV as examples of large values of μ. The limits for $\mu = +500$ GeV and $\mu = -500$ GeV are similar and differ by the hatched region in the figures. Limits are also shown for the intermediate value $\mu = -100\,\mathrm{GeV}$. For large $|\mu|$ the excluded region reaches $(m_{\tilde{e}} + m_{\tilde{q}})/2 = 77\,\mathrm{GeV}$ for a 40 GeV neutralino. This limit worsens at lower neutralino masses, because new decay channels to charginos and next to lightest neutralino open and compete with the direct decay to χ^0_1. In the limit $M_2 \gg M_1$ the charginos and the next to lightest neutralino masses increase leaving only the direct decay channel to χ^0_1 open. In this case the excluded region reaches $(m_{\tilde{e}} + m_{\tilde{q}})/2 = 84$ GeV for a massless neutralino. The excluded region is limited by the small cross section of the process at large $(m_{\tilde{e}} + m_{\tilde{q}})/2$, while for large neutralino masses it is limited by the efficiency that falls to zero as $\Delta m \to 0$. A large variation in $\tan\beta$ results only in slight changes. The limits are shown in c) for $\tan\beta = 1.41$ and in d) for $\tan\beta = 10$ as examples of a small and a large value of $\tan\beta$. The previous limits obtained by H1 are also shown in figure 3 c).

Figure 4 shows the excluded regions in the plane $m_{\tilde{e}}$, $m_{\tilde{q}}$ for fixed values of $m_{\chi^0_1} = 35, 50$ GeV and for different combinations of μ and $\tan\beta$. The excluded area is approximately triangular, defined by a line of constant $m_{\tilde{e}} + m_{\tilde{q}}$ and by two lines parallel to the coordinate axes due to the low efficiency for $\Delta m < 10$ GeV. In figures 4 a) and b) the limits are given for the large μ region ($|\mu| = 500\,\mathrm{GeV}$) and $\tan\beta$ =1.41, 10. The limits obtained at $\tan\beta = 1.41$ and $\mu = -100$ GeV are shown in figure 4 c).

In the range $45 < (m_{\tilde{e}} + m_{\tilde{q}})/2 < 85\,\mathrm{GeV}$ the up quark contribution to the cross section ranges between 70% and 90% because it dominates the parton densities at high-x. The limits on the $\tilde{u}$ mass, assuming all the other squarks to be much heavier, are only ~ 2 GeV below the limit obtained for degenerate squark masses. This is shown as an example in figure 4 d), to be compared with figure 4 c).

8 Comparison with other experiments

A search for the production of selectrons and squarks at HERA has been published by H1 [7]. The present analysis substantially improves these limits due to the seven-fold increase in the integrated luminosity.

Published limits from LEP at $\sqrt{s} = 161 - 172$ GeV exclude selectrons with masses lower than ~ 80 GeV [10]. The present analysis goes beyond this limit for squark masses below ~ 80 GeV. LEP experiments have also reported limits on the stop and on the sbottom squarks [11] of $m_{\tilde{t}}, m_{\tilde{b}} \gtrsim 75$ GeV. The limits given in our analysis are (for $m_{\tilde{e}} \simeq m_{\tilde{q}}$) at the same level as those obtained by combining the LEP limits on $m_{\tilde{e}}$ with those on $m_{\tilde{t}}$

and $m_{\tilde{b}}$ extended to the other squarks, including $\tilde{u}$. Present limits on the mass of the lightest neutralino [31] exclude $m_{\chi_1^0} < 25$ GeV for $\tan\beta \sim 1$ and $m_{\chi_1^0} < 40$ GeV for large $\tan\beta$.

Strong limits on the squark mass have been obtained from the $p\bar{p}$ experiments at the Tevatron [9] and are complementary to those obtained in the present analysis. The Tevatron experiments adopt strong cuts on $\not\!\!P_{\rm t}$ and select final states with many high-$P_{\rm t}$ jets or leptons to exclude the QCD background. Therefore, they are more sensitive to squark cascade decays than to the direct decay $\tilde{q} \to q\chi_1^0$, especially when the mass difference $m_{\tilde{q}} - m_{\chi_1^0}$ is small (~ 20 GeV). On the other hand, the search described in this paper looks only for direct decays and, due to the relatively low cuts on $\not\!\!P_{\rm t}$ (14 GeV) and P_t^h (4 GeV), is sensitive to smaller mass differences. Limits on SUSY are often expressed in terms of the minimal supergravity model (mSUGRA) in which the masses of scalars and fermions are no longer independent parameters [32]. In this model the squarks are always heavier than selectrons and gluinos, and the dominant squark decay is to gluino and quark. In the region where the squark is lighter than the gluino, the Tevatron experiments give limits under more general assumptions than mSUGRA but keep the GUT inspired assumption that links the masses of the neutralinos and the charginos to that of the gluinos. In this framework limits cannot be set on light squarks (~ 80 GeV) when the gluino is too heavy (~ 500 GeV), due to the lack of sensitivity at small $m_{\tilde{q}} - m_{\chi_1^0}$.

The present analysis investigates a different region of the MSSM parameter space, where the gluinos are heavier than the squarks and the squarks masses are independent of the selectron masses, allowing also for $m_{\tilde{q}} \leq m_{\tilde{e}}$. Moreover, no relationships are assumed between $m_{\chi_1^0}$ and $m_{\tilde{g}}$.

9 Conclusions

We have searched for the SUSY process $e^+p \to \tilde{e}^+\tilde{q}{\rm X}\,(\tilde{e}^+ \to e^+\chi_1^0, \tilde{q} \to q\chi_1^0)$ using 46.6 pb^{-1} of data at an e^+p center-of-mass energy of 300 GeV recorded with the ZEUS detector at HERA. One candidate event is found while $1.99^{+0.57}_{-0.84}$ are expected from Standard Model processes. The upper limit on the production cross section times branching ratios is found to be $\sigma \times B < 0.5\,$pb at the 95% CL for mass differences $m_{\tilde{e}} - m_{\chi_1^0}$ and $m_{\tilde{q}} - m_{\chi_1^0}$ greater than 10 GeV. Excluded regions in the MSSM parameter space have been derived. We exclude $(m_{\tilde{e}} + m_{\tilde{q}})/2 < 77\,$GeV at the 95% CL for $m_{\chi_1^0} = 40\,$GeV and large values of the MSSM parameter $|\mu|$. The process is dominated by the $\tilde{u}$ contribution and the exclusion limit is 75 GeV when only the $\tilde{u}$ squark is considered.

Acknowledgements

We appreciate the contributions to the construction and maintenance of the ZEUS detector by many people who are not listed as authors. We especially thank the DESY computing staff for providing the data analysis environment and the HERA machine group

for their outstanding operation of the collider. Finally, we thank the DESY directorate for strong support and encouragement.

References

[1] Yu. A. Gol'fand and E.P. Likhtman, JETP Lett. **13** (1971) 323; D.V. Volkov and V.P. Akulov, JETP Lett. **16** (1972) 438; J. Wess and B. Zumino, Nucl. Phys. **B70** (1974) 39; Nucl. Phys. **B78** (1974) 1.

[2] H.E. Haber and G.L. Kane, Phys. Rep. **117** (1985) 75.

[3] S.K. Jones and C.H. Llewellyn Smith, Nucl. Phys. **B217** (1983) 145; P.R. Harrison, Nucl. Phys. **B249** (1985) 704; T. Bartels, in "Proceedings of the HERA workshop (1987)", edited by R.D. Peccei, DESY 1988, 863; A. Bartl, M. Drees, W. Majerotto, B. Mösslacher, in "Physics at HERA" edited by W.Buchmüller and G.Ingelman, DESY 1992, 1118; T. Kon, K. Nakamura and T. Kobayashi, Phys. Lett. **B223** (1989) 461.

[4] A. Bartl, H. Fraas and W. Majerotto, Nucl. Phys. **B297** (1988) 479.

[5] H. Komatsu and R. Rückl, Nucl. Phys. **B299** (1988) 407; T. Bartels and W. Hollik, Z. Phys. **C39** (1988) 433.

[6] J.L. Lopez, D.V. Nanopoulos, X. Wang and A. Zichichi, Phys. Rev. **D48** (1993) 4029; M. Corradi, in "Future Physics at HERA", edited by G. Ingelman, A. De Roeck and R. Klanner, DESY 1996, 289.

[7] H1 Collaboration, S. Aid et al., Phys. Lett. **B380** (1996) 461.

[8] R. Cashmore et al., Phys. Rep. **122** (1985) 275; P. Schleper, in "Future Physics at HERA", edited by G. Ingelman, A. De Roeck and R. Klanner, DESY 1996, 275.

[9] D0 Collaboration, S. Abachi et al., Phys. Rev. Lett. **75** (1995) 618; CDF Collaboration, F. Abe et al., Phys. Rev. **D56** (1997) 1357; F. Abe et al., Phys. Rev. Lett. **69** (1992) 3439.

[10] ALEPH Collaboration, R. Barate et al., Phys. Lett. **B407** (1997) 377; L3 Collaboration, M. Acciarri et al., CERN-PPE/97-130, accepted by Eur. Phys. J. **C**; OPAL Collaboration, K. Ackerstaff et al., Phys. Lett. **B396** (1997) 301.

[11] ALEPH Collaboration, R. Barate et al., Phys. Lett. **B413** (1997) 431; OPAL Collaboration, K. Ackerstaff et al., Z. Phys. **C75** (1997) 409.

[12] ZEUS Collaboration, "The ZEUS Detector", Status Report 1993, DESY.

[13] N. Harnew et al., Nucl. Inst. Meth. **A279** (1989) 290; B. Foster et al., Nucl. Phys. **B** (Proc. Suppl.) **32** (1993) 181; B. Foster et al., Nucl. Inst. Meth. **A338** (1994) 254.

[14] M. Derrick et al., Nucl. Inst. Meth. **A309** (1991) 77; A. Andresen et al., Nucl. Inst. Meth. **A309** (1991) 101; A. Bernstein et al., Nucl. Inst. Meth. **A336** (1993) 23.

[15] J. Andruszków et al., DESY 92-066 (1992).

[16] GEANT 3.13: R. Brun et al., CERN DD/EE/84-1 (1987).

[17] H. Dreiner and P. Morawitz, Nucl. Phys. **B428** (1994) 31.

[18] M. Glück, E. Reya and A. Vogt, Phys. Rev. **D46** (1992) 1973.

[19] CTEQ Collaboration, H.L. Lai et al., Phys. Rev. **D51** (1995) 4763.

[20] L. Lönnblad, Comp. Phys. Comm. **71** (1992) 15.

[21] T. Sjöstrand, Comp. Phys. Comm. **39** (1986) 347; T. Sjöstrand and M. Bengtsson, Comp. Phys. Comm. **43** (1987) 367.

[22] HERACLES 4.5: A. Kwiatkowski, H. Spiesberger and H.-J. Möhring, Comp. Phys. Comm. **69** (1992) 155.

[23] LEPTO 6.5: G. Ingelman, A. Edin and J. Rathsman, Comp. Phys. Comm. **101** (1997) 108.

[24] DJANGO 6.24: K. Charchula, G.A. Schuler and H. Spiesberger, Comp. Phys. Comm. **81** (1994) 381.

[25] U. Baur, J.A.M. Vermaseren and D. Zeppenfeld, Nucl. Phys. **B375** (1992) 3.

[26] J.A.M. Vermaseren, Nucl. Phys. **B229** (1983) 347.

[27] HERWIG 5.8: G. Marchesini et al., Comp. Phys. Comm. **67** (1992) 465.

[28] AROMA 2.1, G. Ingelman, J. Rathsman and G.A. Schuler, DESY 96-058.

[29] H. Abramowicz, A. Caldwell, and R. Sinkus, Nucl. Inst. Meth. **A365** (1995) 508.

[30] ZEUS Collaboration, J. Breitweg et al., Z. Phys. **C76** (1997) 631.

[31] OPAL Collaboration, K. Ackerstaff et al., Eur. Phys. J. **C2** (1998) 213; DELPHI Collaboration, P. Abreu et al., Eur. Phys. J. **C1** (1998) 1; ALEPH Collaboration, R. Barate et al., Eur. Phys. J. **C2** (1998) 417.

[32] H.P. Nilles, Phys. Rep. **110** (1984) 1; H. Baer and X. Tata, Phys. Rev. **D47** (1993) 2739; J.L. Lopez, D.V. Nanopoulos and A. Zichichi, Phys. Rev. **D53** (1996) 5253.

Process	Expected Events	Stat.	Theor.	Syst.	Total
NC DIS	0.60	± 0.29	± 0.03	$^{+0.06}_{-0.67}$	$^{+0.30}_{-0.73}$
CC DIS	0.18	± 0.07	± 0.01	$^{+0.24}_{-0.10}$	$^{+0.25}_{-0.12}$
W	1.04	± 0.04	± 0.36	$^{+0.09}_{-0.12}$	$^{+0.37}_{-0.38}$
l^+l^-	0.17	± 0.12	± 0.02	$^{+0.17}_{-0.08}$	$^{+0.21}_{-0.14}$
Total	1.99	± 0.32	± 0.36	$^{+0.31}_{-0.69}$	$^{+0.57}_{-0.84}$

Table 1: Background expectation from MC calculations. The table shows the background process, the expected number of events normalized to data luminosity, the statistical error related to the MC statistics, the error due to the theoretical uncertainty on the cross section, the systematic error and the total error.

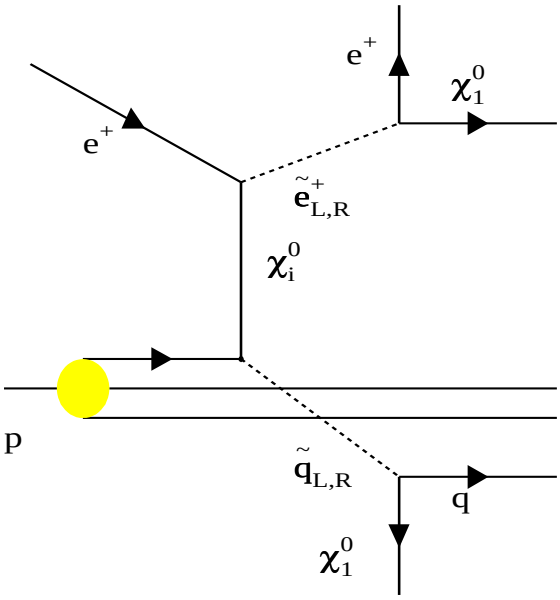

Figure 1: Diagram for the selectron and squark production process.

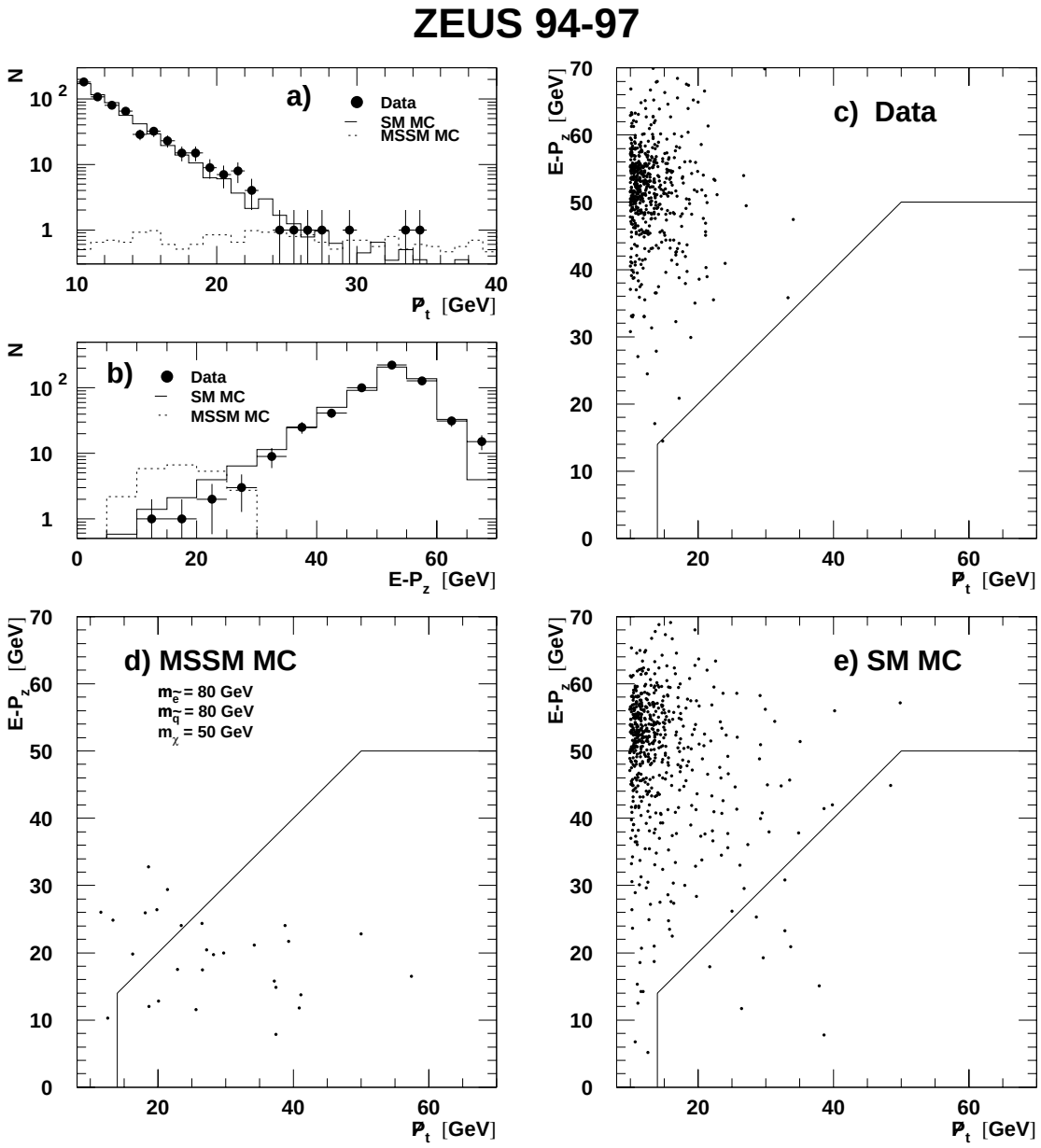

Figure 2: Distributions of events with a selected positron and $\not{P}_t > 10$ GeV, in a) $\not{P}_t$ and b) $E - P_Z$ for data (points), SM background (full line) and a signal example ($m_{\tilde{e}} = 80$ GeV, $m_{\tilde{q}} = 80$ GeV, $m_{\chi_1^0} = 50$ GeV) (dashed line). The distributions of events in the $E - P_Z$ versus $\not{P}_t$ plane are shown in c) for the data, in d) for the MSSM example and in e) for the SM background, where the MC samples are normalized to 5 times the luminosity of the data.

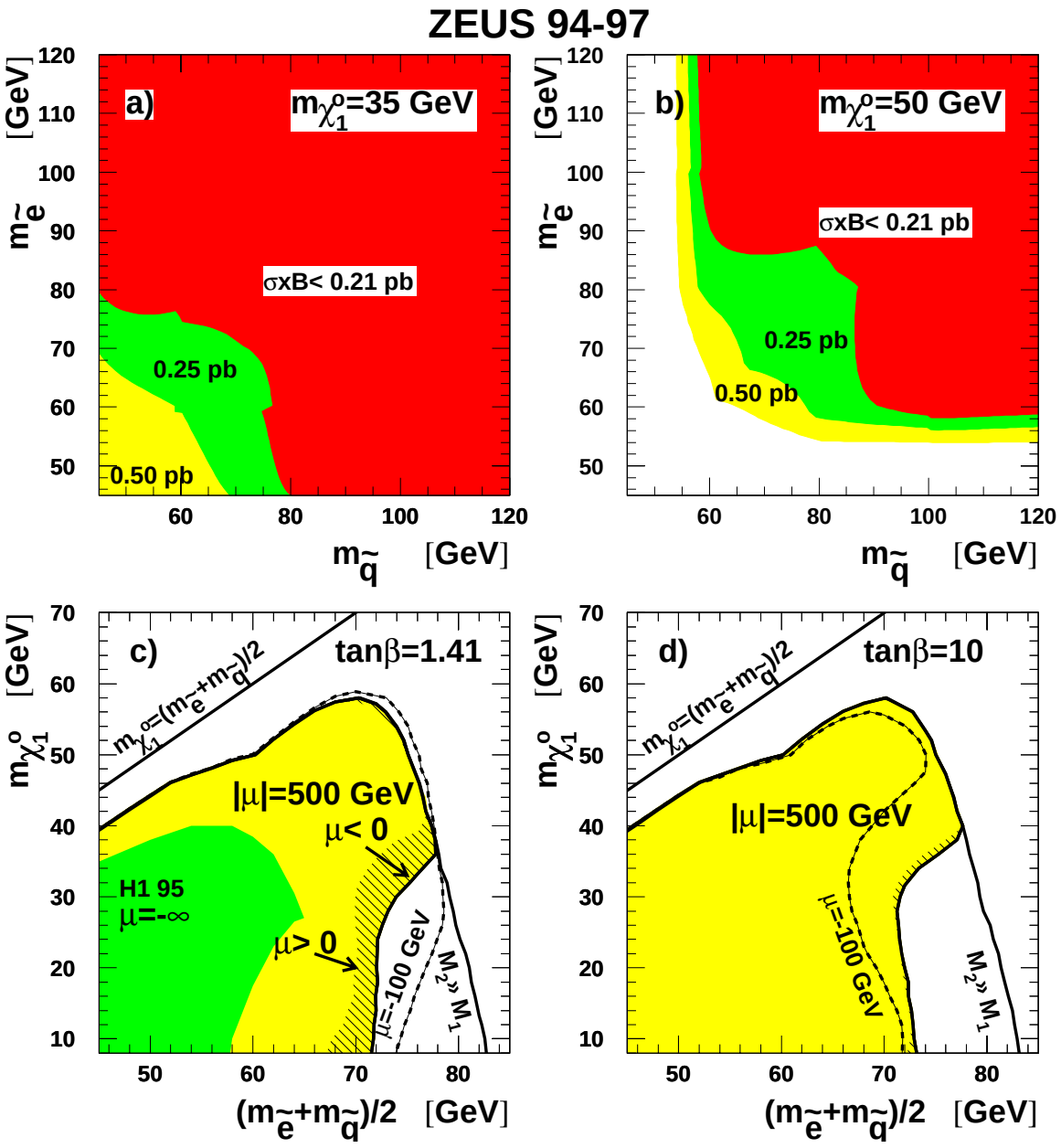

Figure 3: a) and b) 95% CL upper limits on $\sigma \times B$ in the plane defined by $m_{\tilde{q}}$ and $m_{\tilde{e}}$ for two values of the mass of the lightest neutralino: $m_{\chi_1^0} = 35$ GeV in a) and $m_{\chi_1^0} = 50$ GeV in b). c) and d) show the regions excluded at the 95 % CL in the plane defined by $(m_{\tilde{e}} + m_{\tilde{q}})/2$ and $m_{\chi_1^0}$, where limits are evaluated along $m_{\tilde{e}} = m_{\tilde{q}}$ for $\tan\beta = 1.41$ (c)) and for $\tan\beta = 10$ (d)). The grey area is for $|\mu| = 500$ GeV. For $\mu < 0$ the excluded region covers also the hatched grey area. The dashed line is for $\mu = -100$ GeV. These limits are obtained for $M_2 = 2M_1$. If this relation is modified to $M_2 \gg M_1$ the excluded area for $|\mu| = 500$ reaches the full line. The kinematic limit is indicated by the straight line in the upper-left corner. Previous H1 limits from [7] are also shown in c).

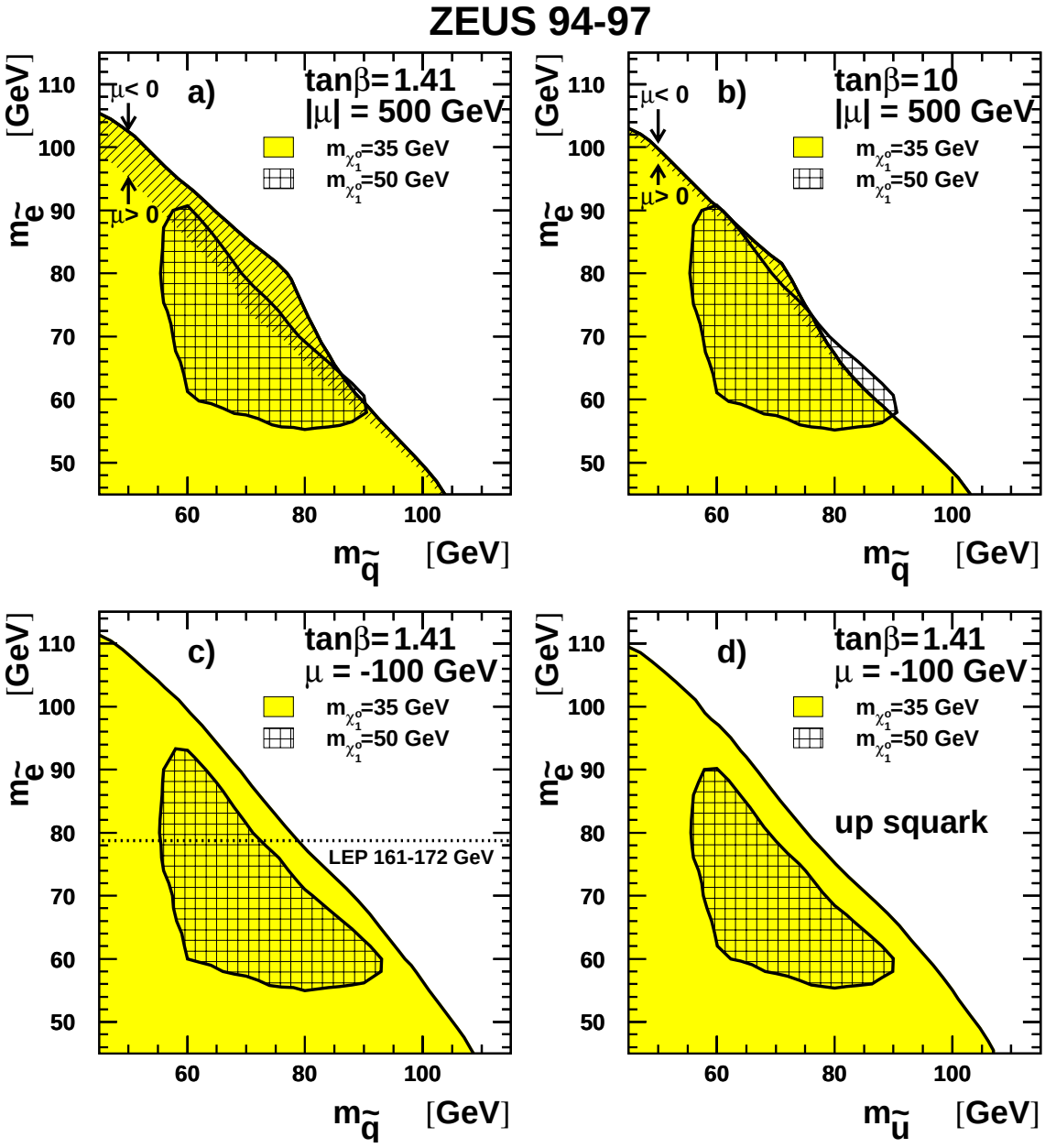

Figure 4: Excluded regions at the 95% CL in the plane defined by the selectron and squark mass, for $m_{\chi_1^0} = 35$ GeV (grey area) and $m_{\chi_1^0} = 50$ GeV (double-hatched area). In a) ($\tan\beta = 1.41$) and b) ($\tan\beta = 10$) the limits are for $|\mu| = 500$ GeV. For $\mu < 0$ the excluded region includes also the single-hatched area. The limits obtained for $\mu = -100$ GeV and $\tan\beta = 1.41$ are shown in c), where LEP limits on $m_{\tilde{e}}$ are also given. The limits for the up squark alone, for the same values of μ and $\tan\beta$, are shown in d).